論 文

Fracture Characteristics of Gray Cast Irons With A or D Type Flake Graphite

Jang-Sik Park

A 또는 D형 片狀 흑연을 갖는 회주철의 파괴특성

朴 長 植

초 록

일방향 응고법으로 주조된 아공정 회주철의 파단면을 주사전자현미경을 이용하여 분석하였다. 회주철에서는 흑연의 형태변화로 인하여 파단면의 형상에 큰 차이점이 유발되었으며, 이와 같이 다양한 파단면의 특성분석을 위하여는 주사전자현미경의 이차전자(secondary electron)를 이용한 입체사진(stereopair micrograph)을 촬영하여 입체적인 관찰을 수행하는 것이 효과적이었다. 일방향으로 응고된 D형 흑연을 갖는 회주철이 A형 회주철에 비하여 열등한 기계적 성질을 갖는 것은 극히 미세한 網狀의 흑연조직과 오스테나이트의 이차 수지상 조직(secondary dendrite arms)의 형성에 기인하는 것으로 확인되었다. 이들 조직은 고 강도의 철상을 거치지 않고 주로 흑연상 주위의 취약한 부분을 통하여만 파괴가 전파되도록 유도함으로써 D형 주철의 파괴강도를 저하시킴이 발견되었다. A형 회주철에서는 조직의 조대함으로 인하여 고 강도의 철조직이 파괴에 참여하게 되어 파괴강도를 높여주는 것으로 확인되었다.

1. Introduction

It has been recognized that the mechanical properties of gray cast irons can be strongly influenced by variations in the solidification structure.[1,2] Solidification of cast irons usually begins with the formation of primary austenite dendrites, followed by the eutectic solidification of the interdendritic liquid. Gray irons result when the interdendritic liguid freezes by the formation of many eutectic cells resulting from the simultaneous precipitation of graphite and austenite at relatively slow cooling rates. The graphite in eutectic cells takes on the form of flakes, and changes its morphology progressively from the coarser type A to the finer type D flake as the cooling rate is increased. The most important variables characterizing the solidification microstructure of gray irons, therefore, include the presence and distribution of primary austenite, the morphology of graphite and the size of eutectic cells. Because of the interdependence and interaction among the structural variables, a large degree of uncertainty still exists concerning their influence on the mechanical properties of gray irons in spite of the considerable research peviously performed.[3,4] In contrast to the general experience that the finer structure increases the strength of a material, it is known that gray irons with the finer type D flake graphite is inferior in both strength and ductility to

홍익대학교 과학기술대학 금속공학과(Department of Metallurgical Engineering, Hong-IK University)

those with the coarser type A flake graphite.[1)]

This study utilized scanning electron microscope(SEM) in order to compare the fracture surface of gray irons containing type A graphite with that of type D gray irons as a first step to understand the reasons for the inferior mechanical properties of the latter. Fracture specimens were prepared using directional solidification technique. In directional solidification, freezing does not proceed by the nucleation and growth of the eutectic cells which are randomly distributed throughout the interdendritic liguid but by the advance of a continuous front in one direction starting near the base of the austenite dendrites, no eutectic cells being formed. With the directionally solidified gray irons, therefore, the effect of graphite morphology, type A versus type D, in the presence of austenite dendrites can be evaluated apart from the celled structures.

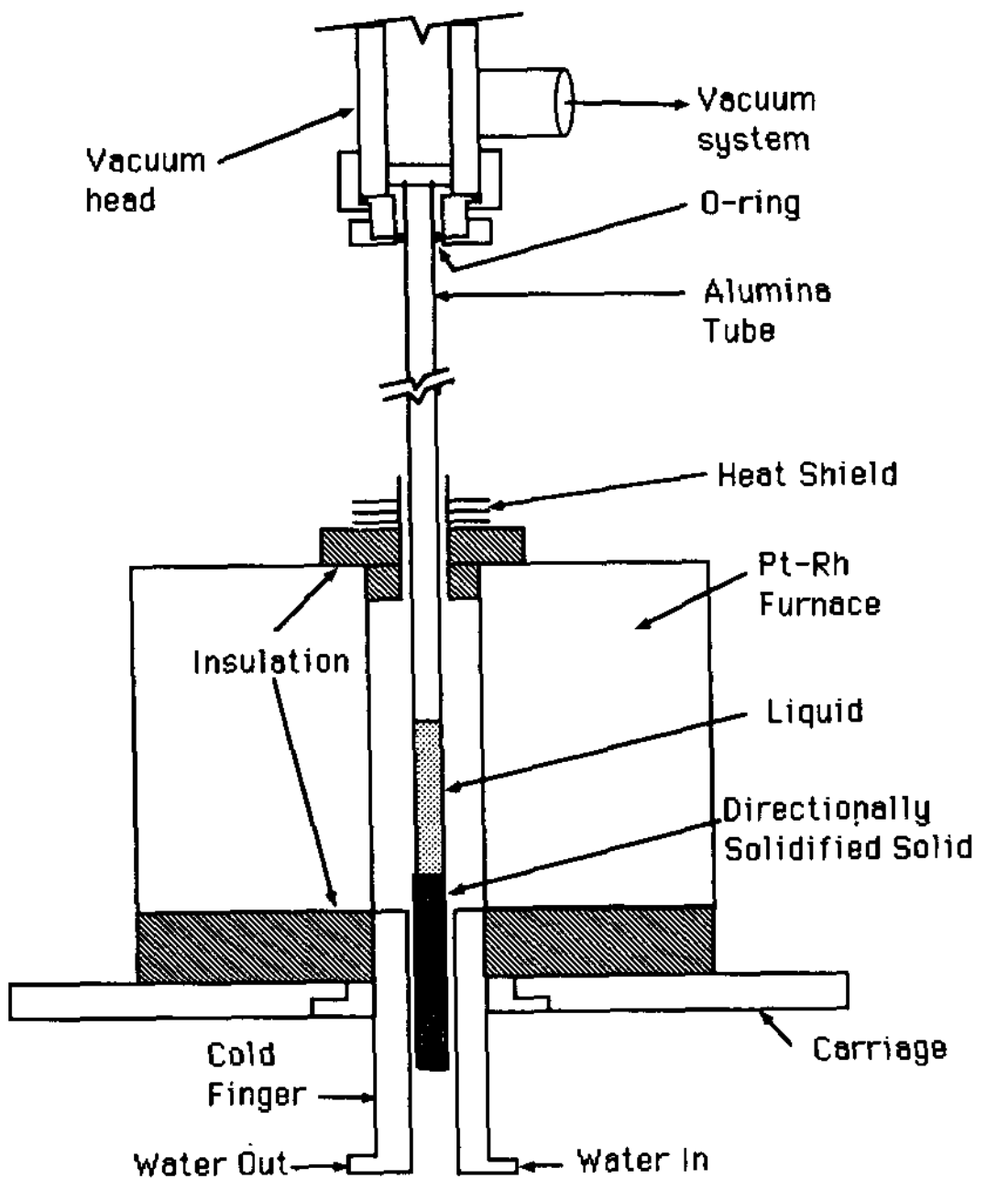

Fig. 1. Schematic diagram of directional solidification arrangement.

2. Experimental Technique

Samples of hypoeutectic composition Fe-3.4 wt.% C-2 wt. % Si-0.1 wt. % Te were directionally solidified in a high purity Al_2O_3 tube of 5 mm I.D. in arrangements shown schematically in Figure 1. The addition of 0.1 wt. % Te here intended to promote the formation of type D graphite at high solidification velocities. The furnace temperature was set at 1450℃ in all the experiments. The details of the directional solidification experiments have already been reported elsewhere.[5)] The directionally solidified 5 mm-diameter samples were longitudinally sectioned and metallographically prepared through the standard series of wet grinding and polishing steps. The microstructures were examined using an optical microscope. Type A and D samples for fracture surface analyses were, then, taken from the parts solidified at 1 um/s and 20 um/s, respectively. Fracture samples about 2 cm long were prepared as shown schematically in figure 2. A V-notch was filed into the sample at right angles to the rod axis, i. e., the growth direction, and fracture occurred by applying an impact on the free end of the sample rod with the other end fixed, producing a pair of mating fracture surfaces. Both surfaces were, then, placed in

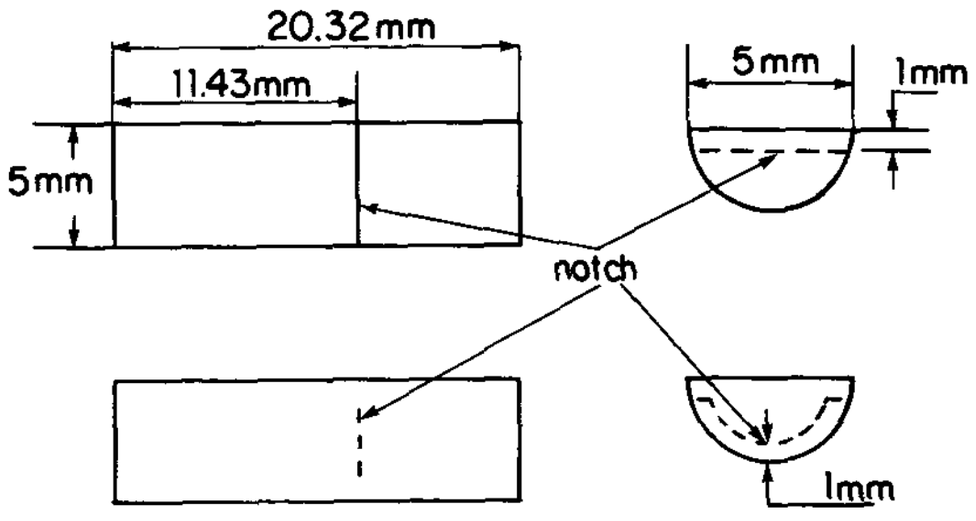

Fig. 2. Schematic diagram of the fracture sample. A v-notch is filed out (a) on the polished flat surface and (b) around the cylindrical surface.

the chamber of a scanning electron microscope(SEM) and secondary electron stereopair micrographs were taken from the area of interest on the fracture surface at two angular positions different by 6 degrees. No attempts were made to take quantitative measurements of the mechamical properties. This study focused on the effect of solidification microstructures(graphite and dendrite) on the fracture characteristics of gray irons. The iron phase of both type A and D samples, initially austenite on solidification, was found to be pearlitic in structure as a result of the transformation in solid state. Fracture was found to occur predominantly along the iron/graphite interface especially in type D gray irons. The fracture through the iron phase was noticeable only in the later stage of the fracturing operation of type A samples. This difference seems to result from the difference in graphite morphologies between type A and D gray irons, independent of the structure of the iron matrix. And the present study did not pursue the effect the structure variation in the iron phase has on the fracture characteristics.

3. Experimental Results

3.1 Gray Irons with Coarse Type A Flake Graphite

An overview of the solidification microstructure is illustrated in Figures 3.a and 3.b, optical micrographs of a gray iron with type A graphite grown at 1 um/s. Figure 3.a, taken from the longitudinal section, shows the coarse type A graphite flakes aligned well along the general solidification direction. The formation of primary dendrites, not evident in the longitudinal section, is easily identified in the transverse section, Figure 3.b, to be the regions where the graphite flakes are absent. Because of the low growth velocity, 1 um/s,

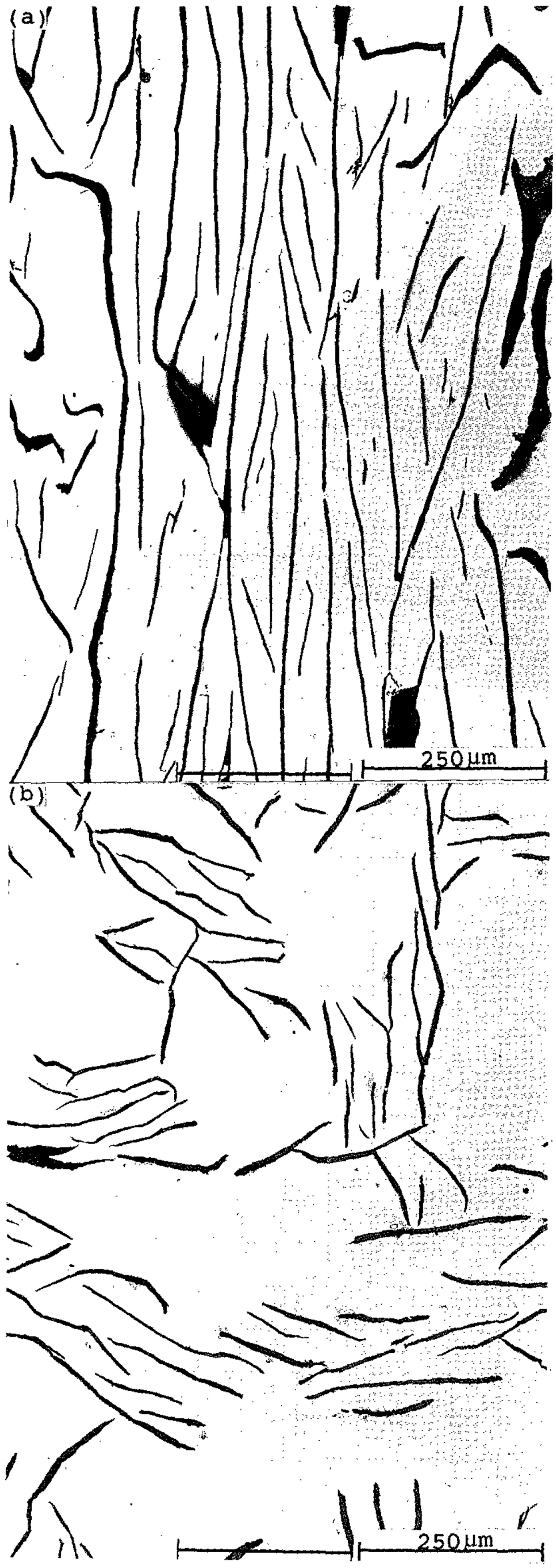

Fig. 3. Optical micrograph of type A graphite

gray irons (a) in a longitudinal section(solidification is upward rate =1um/s) and (b)in a transverse section. As-polished.

it is seen that there are no secondary dendrite arms developed.

To examine the fracture characteristics, secondary electron stereopair micrographs were taken from the fracture surfaces of several samples and analyzed. In all cases, the results were qualitatively the same and the typical result will be presented. Figure 4 presents a low magnification stereopair, taken from the fracture surface of a sample solidified at 1 um/s. It is extremely difficult to obtain a true visualization of the fracture surface unless the stereopair is properly viewed with both eyes, which requires use of a stereoviewer for most people. The stereographic view of the figure reveals that the fracture surface looks like a rugged region with many peaks and valleys. To examine more closely the fracture of the iron and graphite phases, a stereopair micrograph of higher magnification was taken from area A of Figure 4 and presented in Figure 5. The light area in the middle of Figure 5 shows a typical morphology which can be produced by a ductile fracture, and it is apparent that the region represents the fractured iron phase. The thin plates comprising the dark areas, then, must denote the broken graphite flakes. It may be seen from Figure 4 that most of the fracture surface is covered with fairly flat broken graphite flakes with an iron phase occupying a smaller portion of the surface. It seems that each iron phase protruding above the general surface is surrounded by layers of flat graphite flakes, resulting in the rugged mountainous

Fig. 4. Stereopair micrograph of a type A fracture sample. SEM pictures with 6 degree rotation.

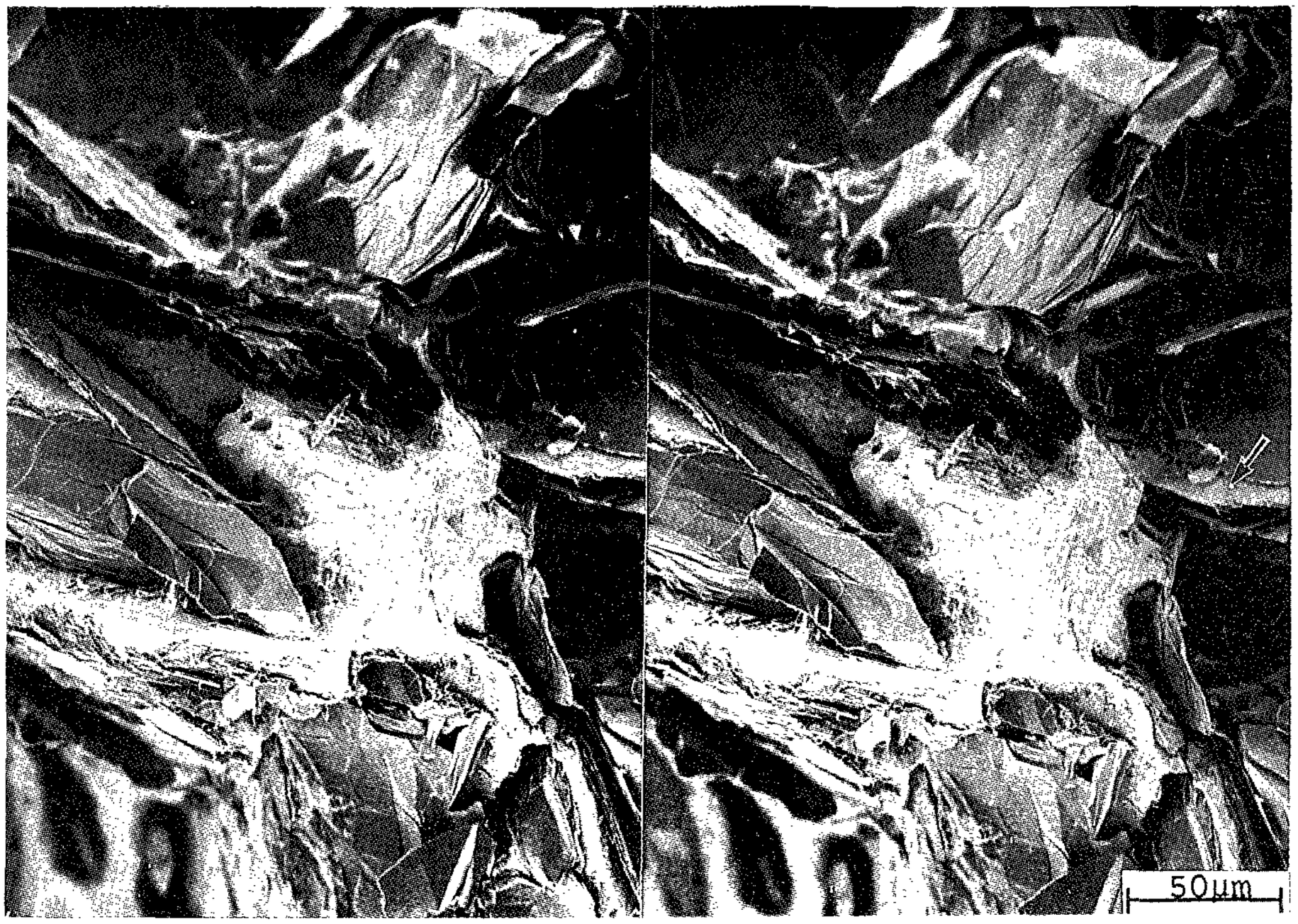

Fig. 5. Higher magnification stereopair micrograph of area A in Fig. 4. SEM pictures with 6 degree rotation.

morphology.

The mechanism producing such a characteristic fracture morphology may be understood from Figure 6, a secondary electron micrograph at the fracture edge, showing the fracture surface at the top and the polished surface at the bottom. The micrograph was taken from the sample solidified at 2.5um/s. The polished surface shows the typical graphite eutectic structures, graphite flakes running through the iron matrix. Fracture is found to occur along the flakes near the fracture edge but no fracture occurs through the iron matrix except in the vicinity of the graphite flakes. This indicates that the graphite flake regions are the weakest point and the first to be affected by the fracturing operation. Careful examination of Figure 5 reveals that the fracture which has occurred along the flake

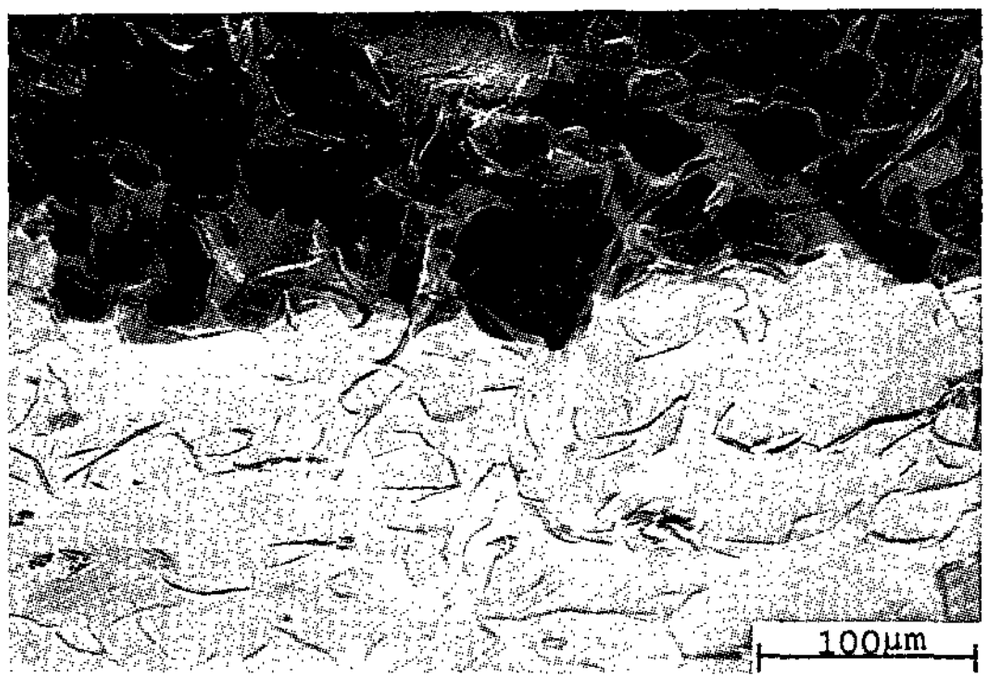

Fig. 6. Secondary electron micrograph of a type A fracture sample showing the fracture surface at the top and the polished surface at the bottom.

regions exposes two types of regions on the surface : flat graphite plate regions and iron/graphite interface regions.

The smooth surfaces of the former indicate

that the graphite flakes, known to consist of many layers of thin plates, have been delaminated by the fracture which occurred parallel to the broad face of the flakes. The broad faces of the graphite flakes are generally held to be basal planes of the hexagonal graphite structure, and delamination along such planes would be expected. The latter, marked by an arrow in Figuer 5, results from the fracture which has occurred right along the boundary between graphite flakes and the iron matrix. It can be seen by combining the results obtained from Figures 4, 5 and 6 that fracture in a gray iron of coarse flake graphite occurs initially right along the graphite flake regions-either through the interior of the graphite flakes or along the iron/graphite boundary-before the fracture of the iron phase is initiated, most probably at the tip of graphite flakes. The final separation is, then, accomplished by the fracture through the interior of the iron matrix region, producing the ductile fracture surface as shown in the middle of Figure 5. The fractured iron matrix region, protruding above the general surface, is surrounded by the broken graphite plates, producing the characteristic rugged morphology as can be seen in Figure 4.

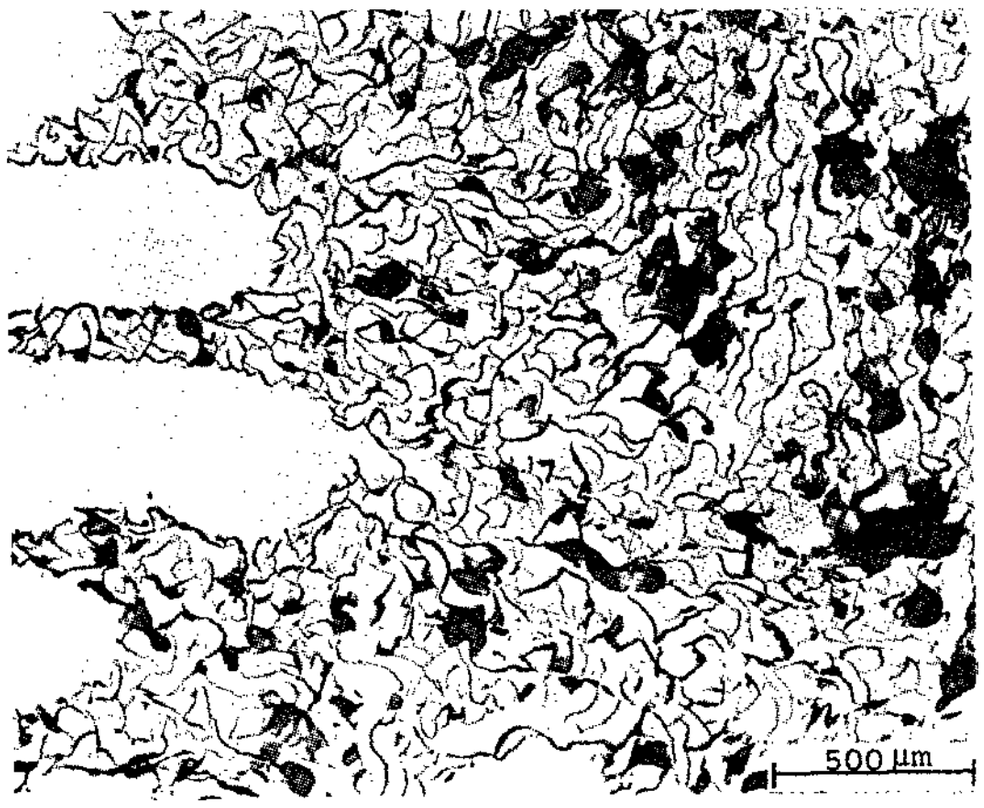

Fig. 7. Optical micrograph of type D gray irons in a longitudinal section. Solidification is upward, rate=20 um/s. As-polished.

3. 2 Gray Irons with Fine Type D Flake Graphite

The microstructure of type D gray iron solidified at 20 um/s is illustrated in Figure 7, an optical micrograph taken from the longitudinal section. The figure shows the presence of secondary dendrite arms on the left as well as the eutectic suructures consisting of graphite flakes embedded in the iron matrix. It is important to note that the flakes shown in Figure 7 are extremely fine, more than an order of magnitude finer than those shown in Figures 3.a and 3.b.

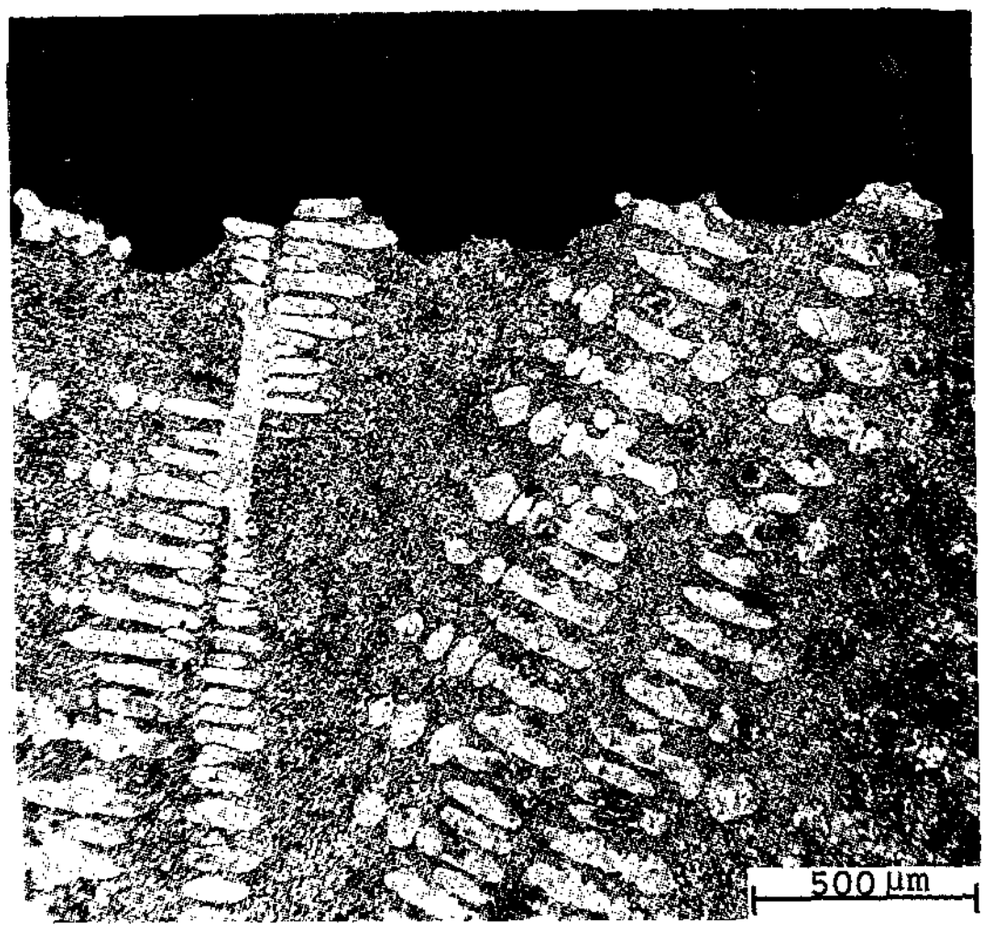

Fig. 8. Optical micrograph of a polished longitudinal section. Fracture surface is at the top. Solidification is upward.

It appears that the fine graphite flakes form a network dividing the iron matrix into many small areas, each of which is almost completely surrounded by the graphite flakes. Figure 8 presents an optical micrograph of the polished longitudinal surface after the sample was fractured at

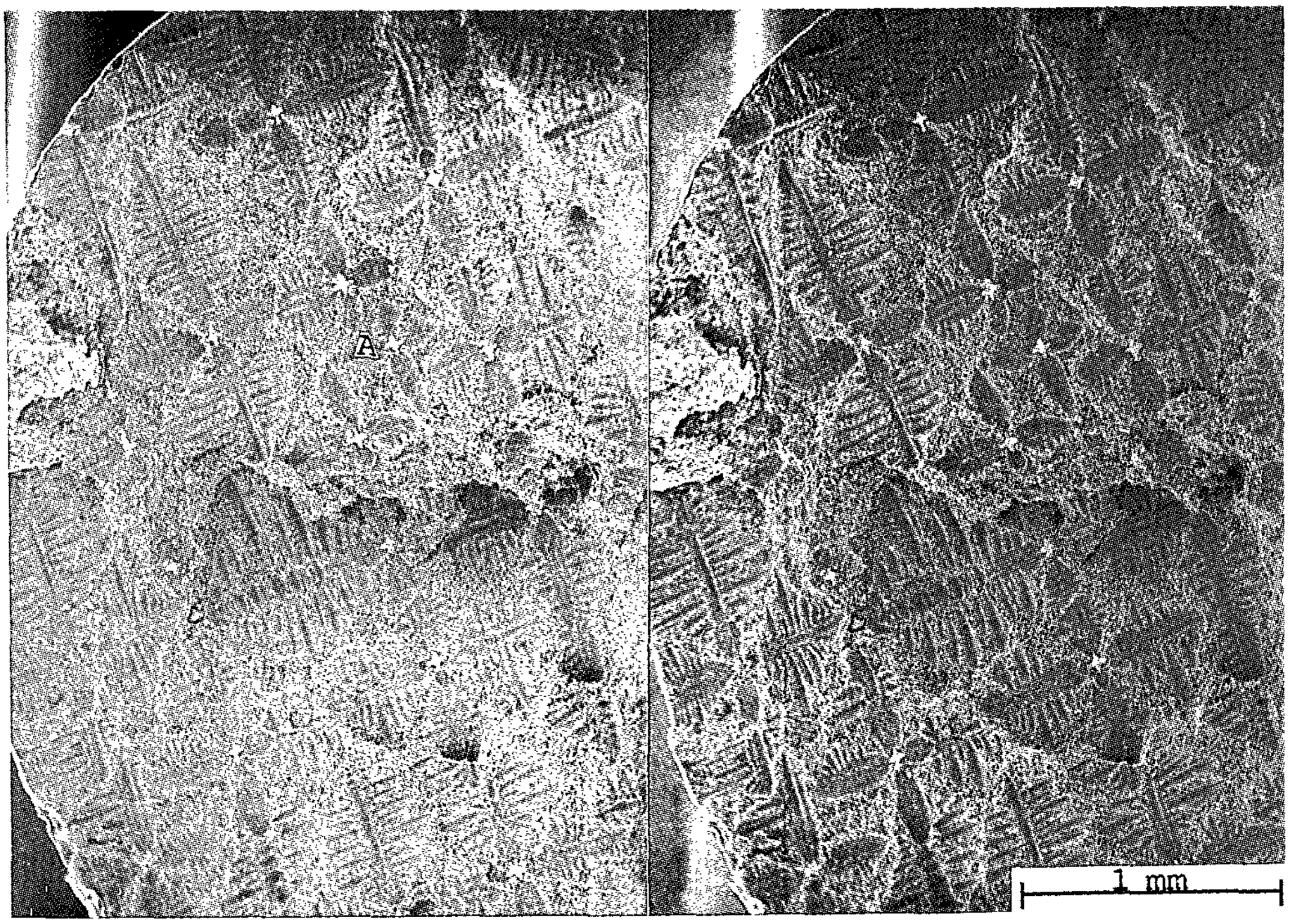

Fig. 9. Stereopair micrograph of a type D fracture sample. SEM pictures with 6 degree rotation.

right angles to the longitudinal direction. The growth of dendrite arms is seen in the figure to occur nearly parallel to the general growth direction. Because of the low magnification, the finer type D graphite flakes are not resolved in the interdendritic region which consists of iron-graphite eutectic. It can be seen in Figure 8 that the fracture surface does not go through the secondary dendrite arms but runs along the interfaces between secondary dendrite arms and the iron-graphite eutectic.

Figure 9 shows a secondary electron stereopair micrograph taken from the fracture surface of a type D gray iron. It is interesting to note that all secondary and tertiary dendrite arms are pulled out of the surface, leaving the cavities on the fracture surface. The detached dendrite arms have been found to remain on the other surface which was mating the one shown in Figure 9. This is in agreement with the result observed in Figure 8 that the fracture has a tendancy to occur along the interfaces between dendrite arms and eutectic structures. The cavities in Figure 9 are seen to fan outward from the small white regions, which represent the primary dendrite arms. Examination of these white regions at high magnification showed that they were iron which had fractured with a characteristic ductile fracture surface. It is apparent from Figures 8 and 9 that, in type D gray irons, the regions between the secondary dendrite arms and the iron-graphite eutectic provide the most probable places for the fracture propagation. This point is further supported by the fact that the surface in Figure 9 contains austenite dendrite arms more than the average amount allowed for the given alloy by the Fe-C phase diagram. This means that the fracture occurs preferentially along

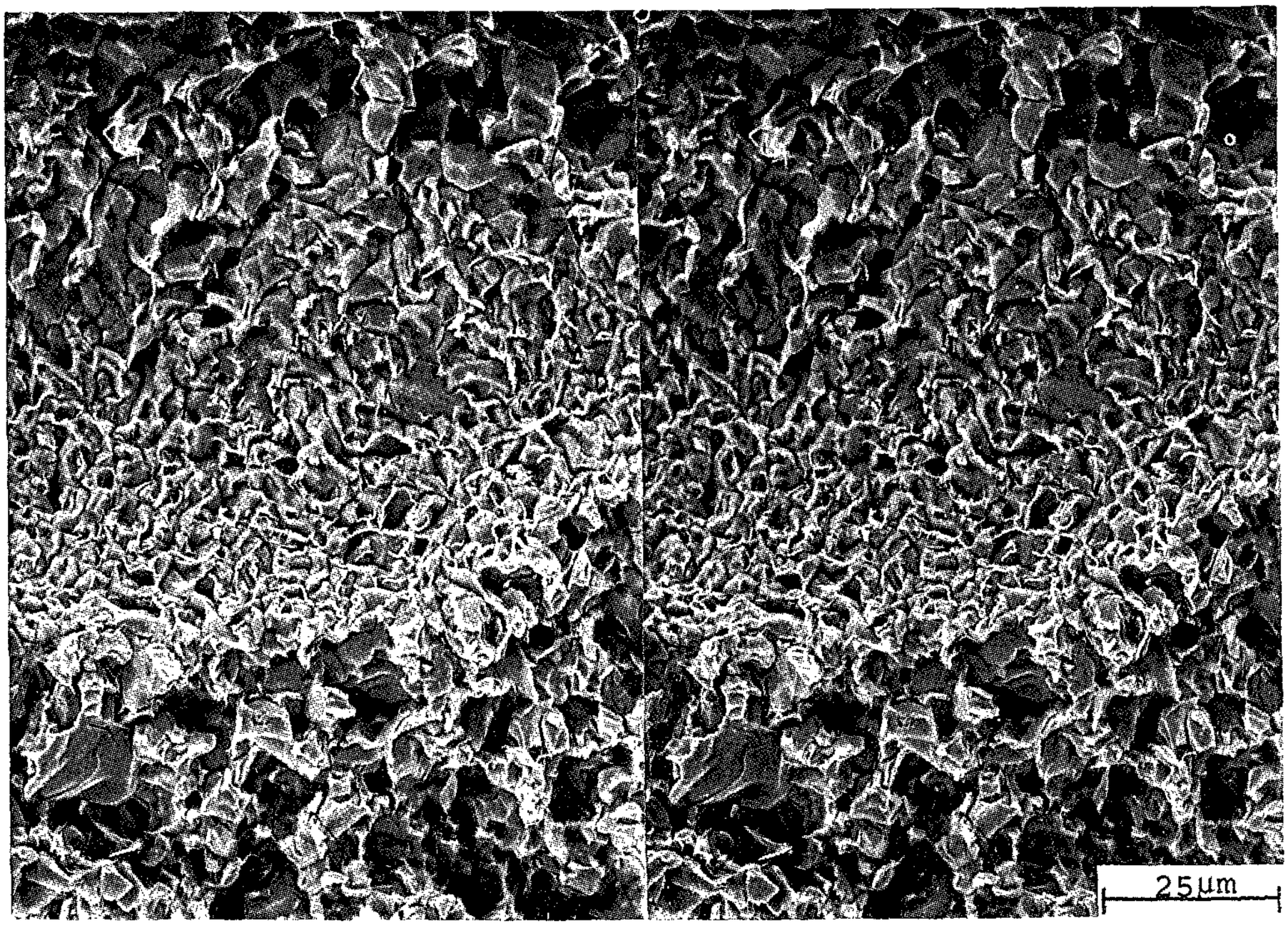

Fig. 10. Higher magnification stereopair micrograph of area A in Fig. 9. SEM pictures with 6 degree rotation.

the regions occupied by the higher density of secondary dendrite arms.

The detailed examination of the fracture surface may be provided by Figure 10, a higher magnification stereopair micrograph of area A in Figure 9. The upper part of the figure shows the area of a cavity left by the impression of one of the secondary dendrite arms and the lower part represents the area of the fractured iron-graphite eutectic formed in the interdendritic region. Examination of both parts using a stereoviewer reveals that the surface consists of many grains and thin wavy flakes protruding over the grains. The origin of the grains and the flakes may be understood from Figure 11, a higher magnification micrograph at the fracture edge showing the polished surface at the top and the fracture surface at the bottom. The polished surface consists of graphite flakes running through the pearlitic iron matrix. The iron matrix appears to be divided into small regions by the graphite flakes. Label A locates one of the divided matrix regions which is about to be separated from the fracture edge. It is evident that the graphite flake regions surrounding the iron matrix provide an easy path for the fracturing process. Labels B1 and B2 locate graphite flakes that have been pulled away from the iron matrix during fracture. It is, therefore, considered that the fracturing operation produces two types of regions : graphite flakes which have been pulled upward from the iron matrix and the surface of the iron matrix regions such as at location C. These iron matrix surfaces all originate from matrix/flake regions, and produce the grains such as those found in Figure 10. The fracture surface in Figure 10 is, therefore, considered to be produced by the fracture which occurs along the iron

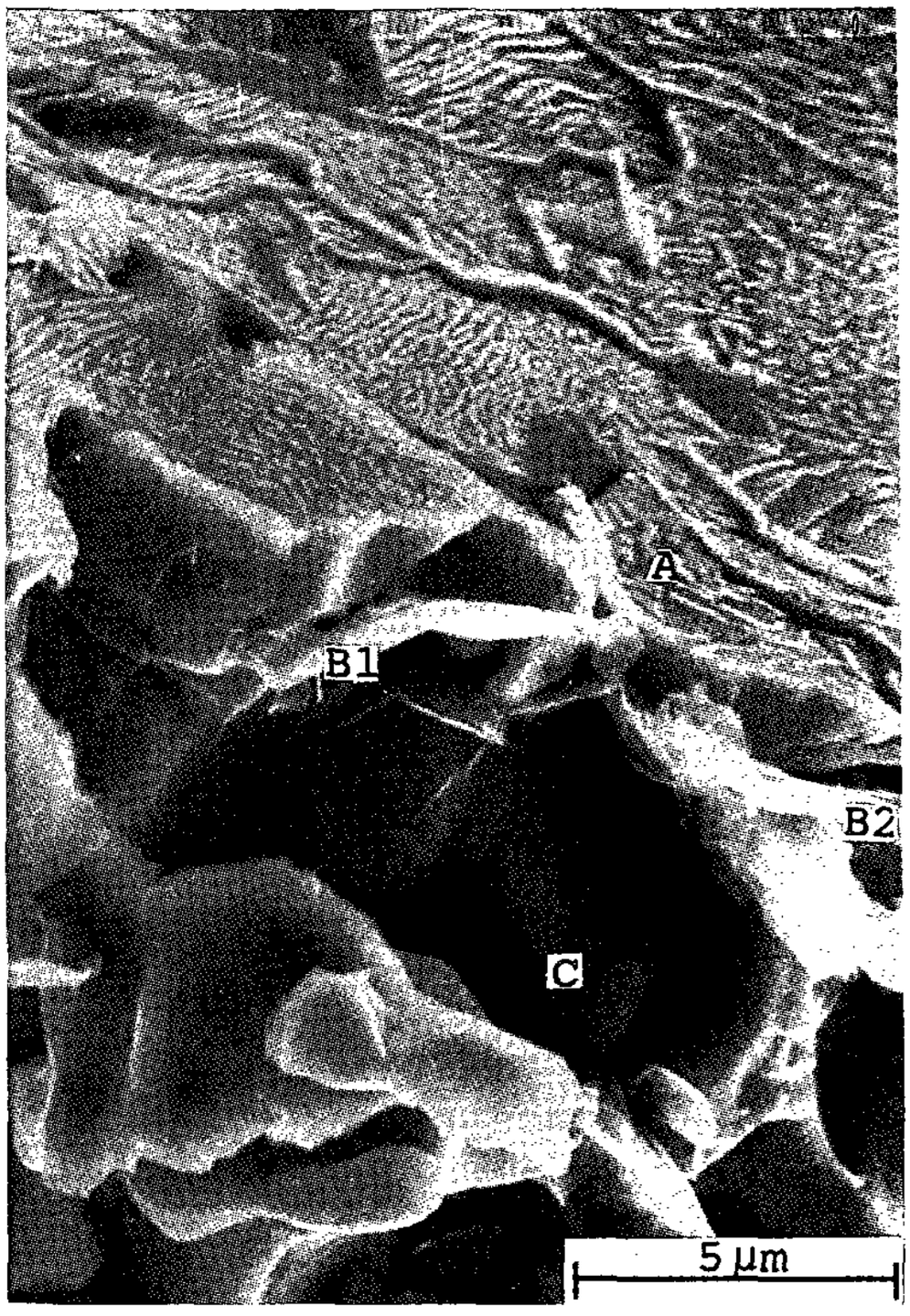

Fig. 11. Secondary electron micrograph of a type D fracture sample showing the ploished surface at the top and the fracture surface at the bottom. Nital etch.

matrix/graphite flake interfaces. Examination of Figure 10 reveals no indication of the characteristic ductile fracture which may occur through the iron matrix. This is in strong contrast to the result obtained from type A graphite gray irons. The iron matrix of the D type gray irons is not fractured through its interior at any point in Figure 9 except for the clearly evident white primary dendrite regions.

4. Discussion

The experimental results show that the fracture of the gray cast irons with coarse type A or fine type D flake graphite occurs initially along the graphite flake regions. The morphology of the fracture surfaces, however, shows a striking difference between the two types of gray irons, as can be verified by comparing Figures 4 and 9. The mechanism making this difference may be understood by examining the behavior of the iron phase in the fracturing process. The iron phase present in gray irons may be developed, during solidification, in two different microstructural elements, dendrite and one of the two constituents comprising eutectic. The relative amount of primary austenite and also that of the iron phase in eutectic structures, which can be formed during solidification, is fixed, in general, by the alloy composition regardless of the graphite morphology. This indicates that the relative amount of the iron and graphite phase is about the same in both the type A and D gray irons examined in this study. But the phases take on different structures, making different responses to the fracturing operation.

The type D gray irons are found to possess two distinctive structural features which make their mechanical properties inferior to those of type A irons. One feature is related to the fineness of the iron-graphite eutectic structure of D gray irons. It may be seen from comparing Figures 3 and 7 that the D flakes are more than an order of magnitude finer than A flakes. Figure 7 shows that the D graphite flakes form fine network-like structures which completely surround the iron matrix. It suggests that fracture through the iron matrix may not be necessary for the completion of fracture. This point is supported by Figure 10 which shows that the fracture surface of a type D gray iron is mostly covered with the broken graphite flakes and the surface of the iron matrix grains, both of which result from the fracture occurring along the graphite flake regions surrounding the iron matrix. Fracture

through the iron phase is found in Figure 9 to occur only at primary dendrite stalks which lie at right angles to the fracture path. Most iron phase present in eutectic structures of D irons does not seem to participate in the fracture process to provide a load-bearing capacity. The situation, however, is different for the coarse type A gray irons. Figures 3. a and 3.b show that the A graphite flakes are much coarser than the type D flakes and do not form such a network as in Figure 7. This suggests that in type A gray irons, fracture through the iron phase in both dendrite stalks and eutectic may be necessary for the complete failure. This is supported by Figure 5. The region in the middle of Figure 5 shows that the fractured iron phase consists of a primary dendrite stalk and several branches attached to it. Figure 3.b, an optical micrograph of the polished transverse section, suggests that the branches are part of the iron phase in eutectic structures. This indicates that the iron phase in type A gray irons may provide a significant load-bearing capacity in the later stage of fracture which has been initiated along the graphite regions.

Another feature responsible for the inferior mechanical property of the D gray iron appears to be related to the development of secondary dendrite arms. Figures 8 and 9 show that the fracture does not go through the secondary dendrite arms in D gray irons. This indicates that the iron phase taking part in the formation of secondary dendrite arms does not provide any stength against fracture. Instead, their development significantly reduces the formation of primary dendrite arms during solidification, reducing portion of the iron phase which may act as a major source of fracture strength in gray irons. In addition, the regions between the secondary dendrite arms and the iron-graphite eutectic provide the most probable places for the fracture propagation. This may be due to the solute enrichment in the liquid ahead of the dendrite arms accompanying their formation in solidification.[6] The network-like structures formed by the extremely fine graphite flakes and the development of secondary dendrite arms are, therefore, considered to be responsible for the inferior mechanical properties of the D type gray cast irons. In type A gray irons, the coarse structures allow the iron phase in both dendrites and eutectics to provide resistance against fracture. In type D irons, however, the fine structures allow only the small portion of the iron phase in primary dendrite stalks to provide the resistance. It is known that the formation of type D flakes is promoted by the action of impurity elements such as S and Te,[5,7] and the secondary dendrite arms develop when the solidification velocity increases. Therefore, strict control on the alloy composition and selection of the slower solidification velocities seem to be necessary to suppress formation of the mechanically inferior type D gray cast irons.

5. Conclusions

1. Fracture of the directionally solidified gray irons with type A or D graphite occurs initially along the graphite flake regions.

2. The coarse structure of type A gray irons allows the iron phase to act as a major source of their fracture strength.

3. The inferior mechanical properties of type D irons appear to result from the network-like structures formed by the extremely fine graphite flakes and the development of secondary dendrite arms. The network structure enables the failure to be completed by the fracture occurring mostly along the graphite regions without much need of fracture through the iron matrix except at primary dendrite stalks. The development of secondary dendrite arms

reduces the fracture strength of D gray irons by reducing portion of the iron phase which can provide load-bearing capacity and also by producing the most probable places for the fracture propagation.

Acknowledgements

This work was funded by the research -support plan of Hong-Ik university for the new faculty members.

References

1. G.F. Ruff and J. F. Wallace : AFS Trans., Vol. 84(1976) 705.
2. G.F. Ruff and J. F. Wallace : AFS Trans., Vol. 84(1977) 179.
3. Y. Kuroda and H. Takada : AFS Cast Met. Res., Vol.3(1970) 63.
4. A. G. Glover and G. Pollard : J. Iron and Steel Inst., Feb. (1971) 138.
5. J. D. Verhoeven, J. S. Park and L. L. Jones : Met Trans. A, Vol. 20A (1989) 1867.
6. J. D. Verhoeven, A. J. Bevolo and J. S. Park : Met. Trans. A, Vol.20A(1989) 1875
7. J. S. Park : Ph. D. Thesis, Iowa State Univ., Aug. (1990).